Stanford Exploration Project, Report 75, November 17, 1997, pages 437–458

Stanford Exploration Project, Report 75, November 17, 1997, pages 437–458

Dip-Moveout processing: A Tutorial. DMO basics and DMO by Fourier transform

Alexander M. Popovici[1]

keywords: *DMO, Fourier transform, velocity, NMO*

ABSTRACT

As a Teaching Assistant (TA) for Jon Claerbout's class I prepared several lectures on DMO. Two of them appear polished enough to be included in this report. The first part explains the DMO correction in simple, geometrical terms and justifies its place in the imaging processing sequence. The second part deals with DMO by Fourier methods.

INTRODUCTION

The Dip Moveout correction (DMO) is an intermediate processing step which when applied together with the Normal Moveout correction (NMO) transforms a constant-offset section into a zero-offset section. There are many benefits to introducing the DMO processing step. Perhaps the best overall quality is the fact that it is a very robust process. It needs very few parameters and almost always improves the output section.

By applying the succession of DMO, NMO, stacking and zero-offset migration we replace the more expensive sequence of prestack migration for each offset and stacking. However the migration to zero-offset is not the only improvement that DMO delivers to the seismic section. A list of DMO promises is given by Deregowski (1986) and includes improvement of velocity analysis, dead traces interpolation, improvement of cross-line ties, steep dip coherent noise attenuation, improvement of the signal to noise ratio, diffraction preservation, etc. These beneficial effects will be discussed further.

The need for DMO

The need for Dip Moveout appeared from the problem of stacking traces that share the same Common-Mid-Point (CMP). Figure **??** shows the geometry of a CMP section

[1]**email:** not available

over a flat layer. In a CMP section, traces are sorted so they share the same mid-point for different locations of the source and receiver. In this configuration when only flat layers are present, the reflections come from a single point situated under the CMP.

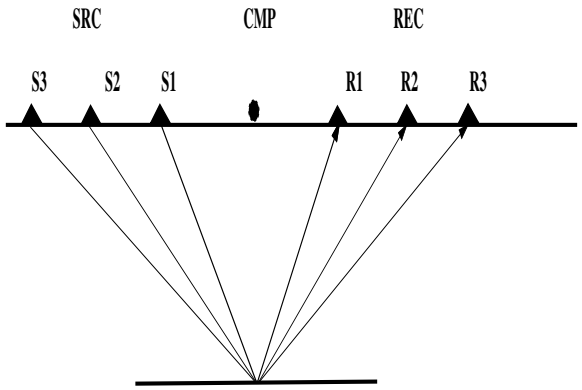

Figure 1: Geometry for CMP gather over a flat layer.

Figure ?? depicts the geometry of a CMP section over a dipping layer. In this case the reflections do not come from the same point, but are moving updip as the offset between source and receiver increases.

The CMP Stacking assumes that reflections come from horizontal layers. Under this assumption the Normal Moveout correction (NMO) flattens the hyperbolas in a CMP gather to horizontal lines. After NMO, traces belonging to the same CMP are summed together (stacked) to enhance the reflected signal and to attenuate the noise.

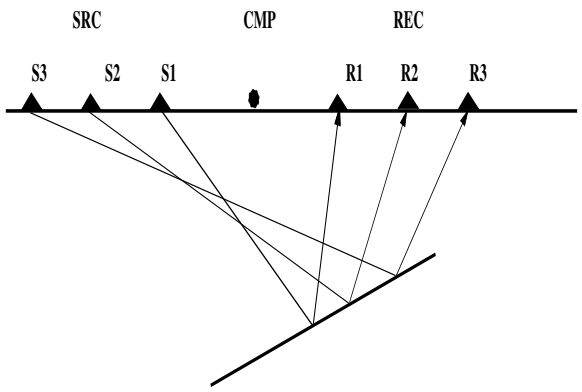

Figure 2: Geometry for CMP gather over a dipping layer.

Problems appear when multiple dipping events are present in a section. If we combine Figures ?? and ?? for multiple CMPs we obtain Figure ??a. In Figure ??a we combine the geometry in Figures ?? and ?? for multiple Common-Mid-Points. Each hyperbola corresponds to a CMP section over a dipping layer and a flat layer. As the CMP moves updip, the hyperbolas corresponding to the dipping layer appear closer to the surface while the ones corresponding to the flat layer are unchanged.

A dipping reflector in a CMP section (see Figure ??a) produces a reflection hyperbola as it will be proven later. The NMO velocity necessary to flatten the hyperbolas originating from reflections on the dipping layer is higher than the real velocity.

Figure ??a shows several CMP gathers containing reflections from a dipping layer and from a horizontal layer. After NMO with the **real velocity** the hyperbolas corresponding to the flat layer become straight lines (Figure ??b) and after stacking (Figure ??c), the horizontal event is preserved at the expense of the dipping event. In Figure ??b NMO is performed with a **higher velocity** which is necessary to flatten the hyperbolas corresponding to the dipping event. After stacking (Figure ??c) the dipping event is preserved at the expense of the horizontal layer. It is obvious that the NMO correction with a single velocity combined with CMP stacking acts as a dip filter. The result is a degradation of the final image when conflicting dips are present.

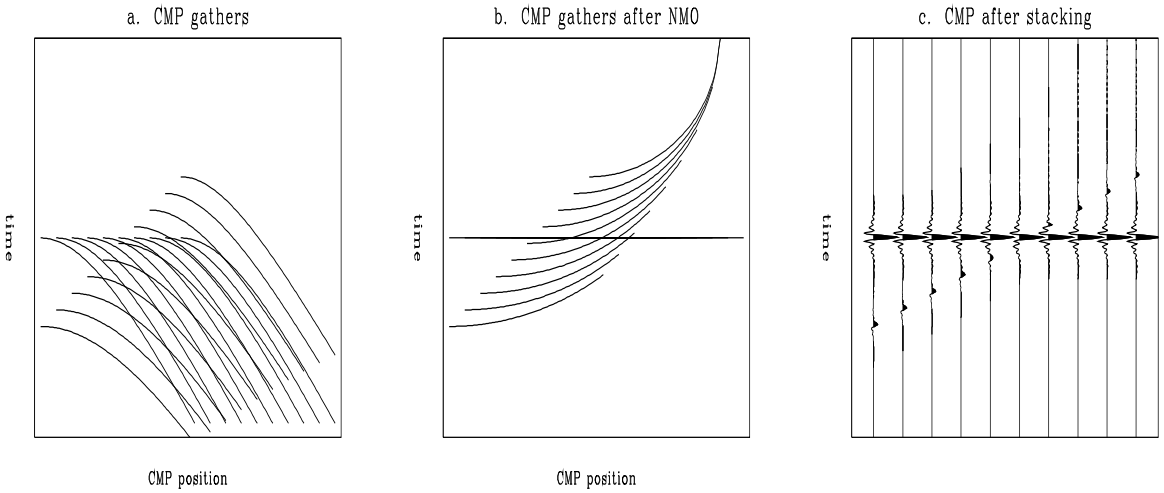

Figure 3: The effect of CMP stacking with real velocity on **dipping reflectors**.
a. Several CMP gathers for a flat layer and a dipping layer.
b. The CMP gathers after NMO with medium velocity (v_{real}); the hyperbolas from the horizontal event are flattened.
c. Traces after stacking for the same CMP.

The NMO velocity

Figure ?? shows a dipping reflector and the position of the source, geophone and CMP. The constant-offset traveltime from the source at point **A** to the receiver at point **B** is represented by the segments **AR**+**RB**. The zero-offset traveltime from the CMP to the reflector and back is given by the segment **FG**. The dipping reflector serves as the axis of symmetry for the figure.

For the geometry in Figure ?? we have

$$\mathbf{AC} = \mathbf{AR} + \mathbf{RB} = vt_h$$

where v is the velocity of the medium and t_h is the shot-receiver traveltime. The segment **FG** (which has the length of the zero-offset raypath) is equal to the segment **AE**. From Figure ??

$$\mathbf{FG} = (\mathbf{AD} + \mathbf{BC})/2 = \mathbf{BC} + \mathbf{ED} = \mathbf{AE}.$$

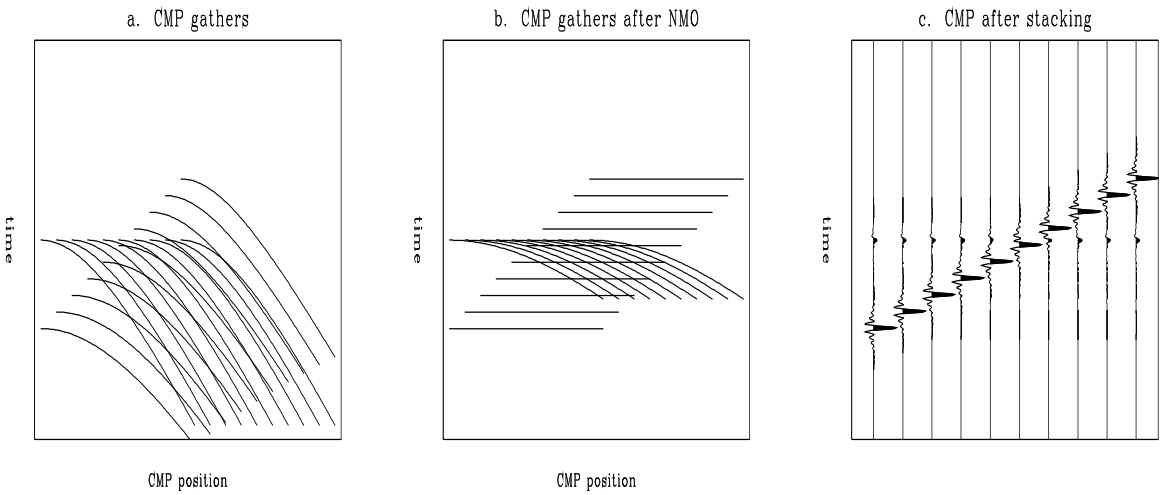

Figure 4: The effect of CMP stacking with velocity ($v_{nmo} = v_{real}/\cos\theta$) on **horizontal reflectors**.
a. Several CMP gathers for a flat layer and a dipping layer.
b. The CMP gathers after NMO with higher velocity; the hyperbolas from the dipping event are flattened.
c. Traces after stacking for the same CMP.

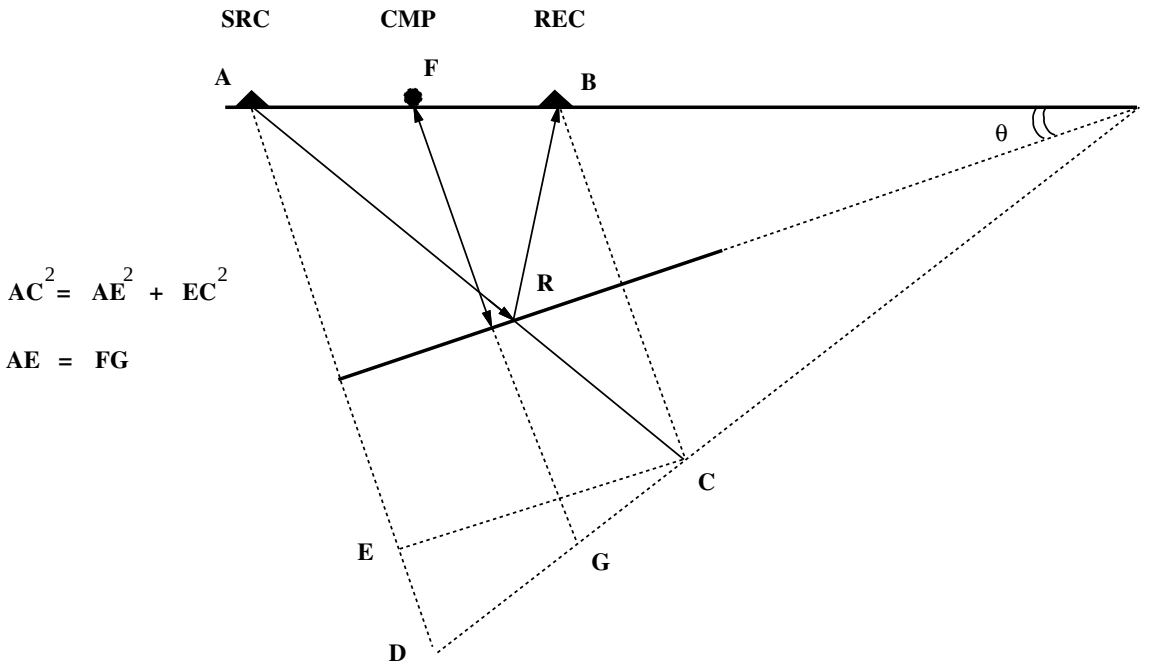

Figure 5: A dipping reflector in a constant velocity medium. The dipping angle is θ. The raypath from the source to the receiver is sketched by the segments **AR** and **RB**. The zero-offset raypath is equal to the segment **FG**.

From the triangle $\triangle\mathbf{AEC}$ we have

$$\mathbf{FG}^2 = \mathbf{AE}^2 = \mathbf{AC}^2 - \mathbf{EC}^2 = (vt_h)^2 - (2h\cos\theta)^2, \tag{1}$$

where θ is the angle of the dipping reflector and $2h$ is the distance between source and receiver. Finally, by dividing the segments with the velocity we have the zero-offset traveltime from the CMP to the reflector:

$$t_0^2 = t_h^2 - \left(\frac{2h\cos\theta}{v}\right)^2 = t_h^2 - \left(\frac{2h}{v_{nmo}}\right)^2. \tag{2}$$

From equation (2) we easily see that the expression for t_h is a hyperbola, with the top at t_0. The NMO velocity necessary to flatten the hyperbola for a dipping reflector is

$$v_{nmo} = \frac{v}{\cos\theta}. \tag{3}$$

DMO and NMO

The Dip Moveout correction (DMO) is in fact an extension to the NMO correction when dips are present. In the presence of only horizontal layers NMO tries to correct the effect of the offset and transform all the constant-offset section into zero-offset section. You can understand the DMO correction as doing exactly the same thing not only for horizontal events but also for dipping events. DMO is an intermediate processing step which attempts to position the conflicting dips in the correct zero-offset location such that after NMO, CMP stacking will not attenuate crossing events.

These concepts are all formulated for a constant velocity medium. For a variable velocity medium the transformation from constant-offset to zero-offset performed by NMO combined with DMO can not be split into two separate processes; instead it forms a single step process called Migration to Zero-Offset (MZO). In constant velocity media $MZO = NMO \cdot DMO$.

To define the parameters involved in the DMO correction we need to analyze the kinematics of the constant-offset reflection of a dipping layer. For a horizontal layer, the reflection point is situated right under the location of the common-midpoint (CMP). For the dipping layer sketched in Figure **??** the reflection point for the source-receiver ray is **R**. This point is positioned updip relative to the intersection **O** of the zero-offset ray from the common-midpoint **F** with the dipping reflector.

In a constant-offset section the trace corresponding to a source positioned at point **A** and a receiver positioned at point **B** is placed in the location of the CMP. However in a zero-offset experiment the reflection point **R** is observed from the surface position **J**. Migration to zero-offset ($NMO \cdot DMO$) is the transformation which relocates a reflection point as seen in constant-offset to a place corresponding to the reflection point as seen in zero-offset.

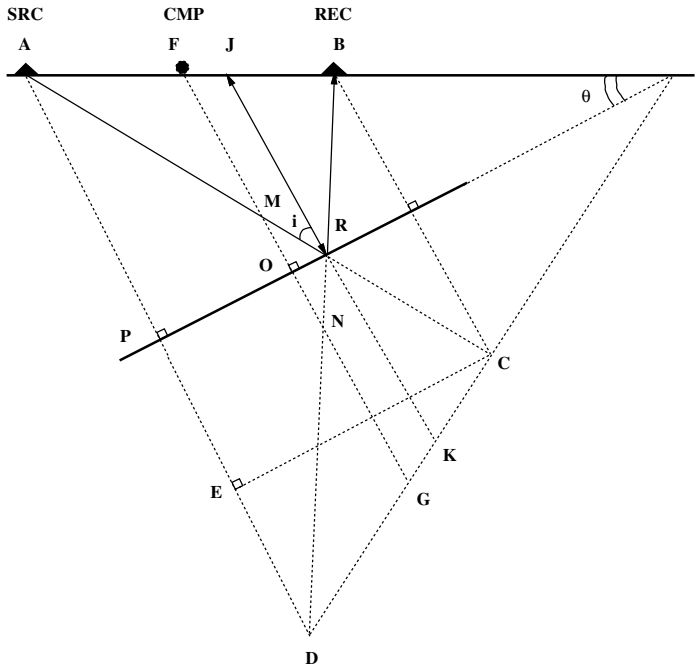

Figure 6: DMO kinematics. A dipping reflector in a constant velocity medium. The dipping angle is θ. The raypath from the source to the receiver is sketched by the segments **AR** and **RB**. The reflection point **R** is seen in the zero-offset case from the surface point **J**. The zero-offset raypath from **J** is equal to the segment **JK**. The incidence angle at **R** is i.

In order to define the operator we have to calculate the time correction and the surface coordinate correction to transform a constant-offset section into a zero-offset section. In Figure **??** the segment **JR** represents the zero-offset ray from the reflection point **R**. The segment **FJ** represents the surface correction from the CMP to the real zero-offset position of both the source and receiver. We can calculate the surface correction and the traveltime correction using some elementary geometry.

The source-receiver traveltime t_h corresponds to the ray path **ARB**. The velocity of the medium is v and the constant-offset traveltime is

$$t_h = \frac{(\mathbf{AR} + \mathbf{RB})}{v}.$$

The segment **AB** represents the offset between the source and receiver and we have

$$\mathbf{AF} = \mathbf{FB} = \frac{\mathbf{AB}}{2} = h.$$

The segment **AC** is equal to **AR** +**RB** and therefore $\mathbf{AC} = vt_h$.

From Figure **??** we observe that the most important equation relating the angle of the dipping reflector and the incidence angle of the constant-offset raypath is

$$2h\cos\theta = vt_h \sin i = \mathbf{EC}, \tag{4}$$

where θ is the dipping angle of the reflector and i is the incident angle of the constant-offset raypath at the reflection point **R**. From equation (4) we have

$$\cos i = \frac{1}{vt_h}\sqrt{(vt_h)^2 - (2h\cos\theta)^2}.$$

To calculate the segment $x_0 = \mathbf{FJ}$ which is the DMO surface correction we note that

$$x_0 = \frac{\mathbf{OR}}{\cos\theta}$$

and

$$\mathbf{OR} = \mathbf{MO}\tan i.$$

The segment **MN**= 2**MO** is easily calculated as half the difference between the bases of the trapezoid **ABCD**. We have

$$\mathbf{MO} = \frac{\mathbf{MN}}{2} = \frac{\mathbf{AD} - \mathbf{BC}}{4} = h\sin\theta \tag{5}$$

and finally

$$x_0 = h\sin\theta\frac{\tan i}{\cos\theta} = \frac{2h^2\sin\theta}{\sqrt{(vt_h)^2 - (2h\cos\theta)^2}}. \tag{6}$$

Knowing segment **FJ**, the zero-offset traveltime given by the segment **JK** is calculated as

$$\mathbf{JK} = \mathbf{FG} - 2\mathbf{FJ}\sin\theta.$$

The segment **FG** is expressed in equation (1)

$$\mathbf{FG} = \sqrt{(vt_h)^2 - (2h\cos\theta)^2}.$$

Therefore we have

$$t_0 = \frac{\mathbf{JK}}{v} = \frac{(vt_h)^2 - (2h)^2}{v\sqrt{(vt_h)^2 - (2h\cos\theta)^2}}. \tag{7}$$

We have obtained the parametric equations defining the $NMO \cdot DMO$ operator in constant velocity media:

$$\begin{cases} x_0 = \dfrac{2h^2\sin\theta}{v\sqrt{t_h^2 - \frac{4h^2\cos^2\theta}{v^2}}} \\ \\ t_0 = \dfrac{t_h^2 - \frac{4h^2}{v^2}}{\sqrt{t_h^2 - \frac{4h^2\cos^2\theta}{v^2}}}. \end{cases} \tag{8}$$

The formulas in equation (**??**) tell us where an event from a constant-offset section is moved in a zero-offset section when the dip is known. However we will see later that the dip does not have to be known to correctly apply the DMO operator. Figure **??** shows the variation of t_0 and x_0 for a whole range of dips. For a zero dip we have

$$\begin{cases} x_0 = 0 \\ \\ t_0 = \sqrt{t_h^2 - \left(\dfrac{2h}{v}\right)^2} \end{cases}$$

which is just the NMO correction.

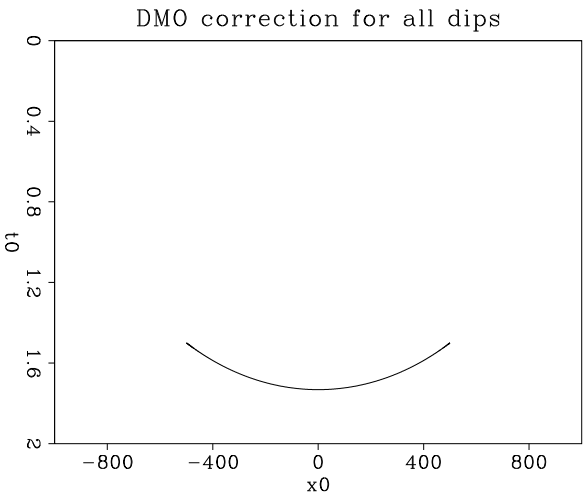

Figure 7: The distribution of the DMO correction for all dips ($\frac{-\pi}{2} \leq \theta \leq \frac{\pi}{2}$).

How DMO works

The goal of the $NMO \cdot DMO$ processing step is to transform a constant-offset section into a zero-offset section. We can conceive any structure (or depth model) as composed of independent diffractors. This is the commonplace assumption for Kirchhoff migration. By summing the contributions from all the diffractors we can obtain our constant-offset section. Following this hypothesis it is interesting to examine the behavior of a single diffraction curve in constant-offset. Figure **??** shows a **constant-offset** diffraction curve together with a **zero-offset** diffraction curve which is actually a hyperbola. The aim of the $NMO \cdot DMO$ step is to transform the former into the latter.

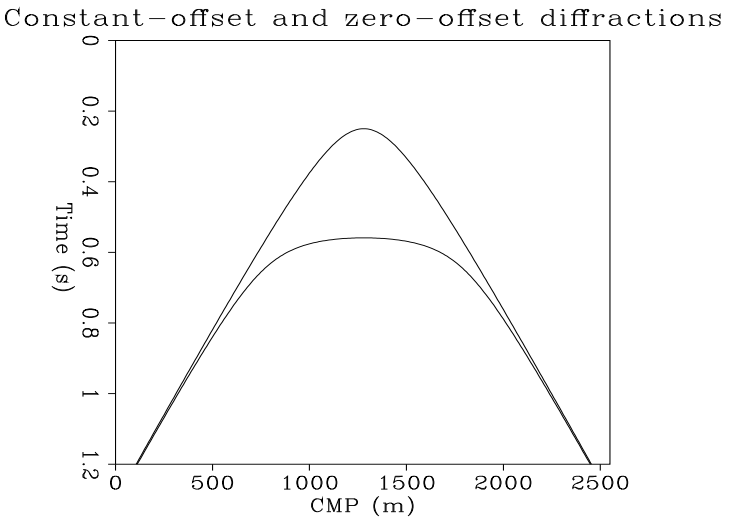

Figure 8: Zero-offset hyperbola and the constant-offset diffraction curve.

Figure **??** shows the kinematics of the $NMO \cdot DMO$ operator; each point along the constant-offset diffraction curve is spread along an operator similar to the one shown in Figure **??** and using equation (8). The result of this operation is displayed on the right side in Figure **??**. The artifacts at the top of the figure are due to the constant amplitude assigned along the DMO curve. In reality the amplitude along the DMO curve is tapered toward the end of the operator, as will be shown later.

Problem 1.

Demonstrate that for the geometry presented in Figure **??** we have the following equality:

$$\frac{\mathbf{AD}}{\mathbf{FG}} = \frac{\mathbf{JK}}{\mathbf{BC}}.$$

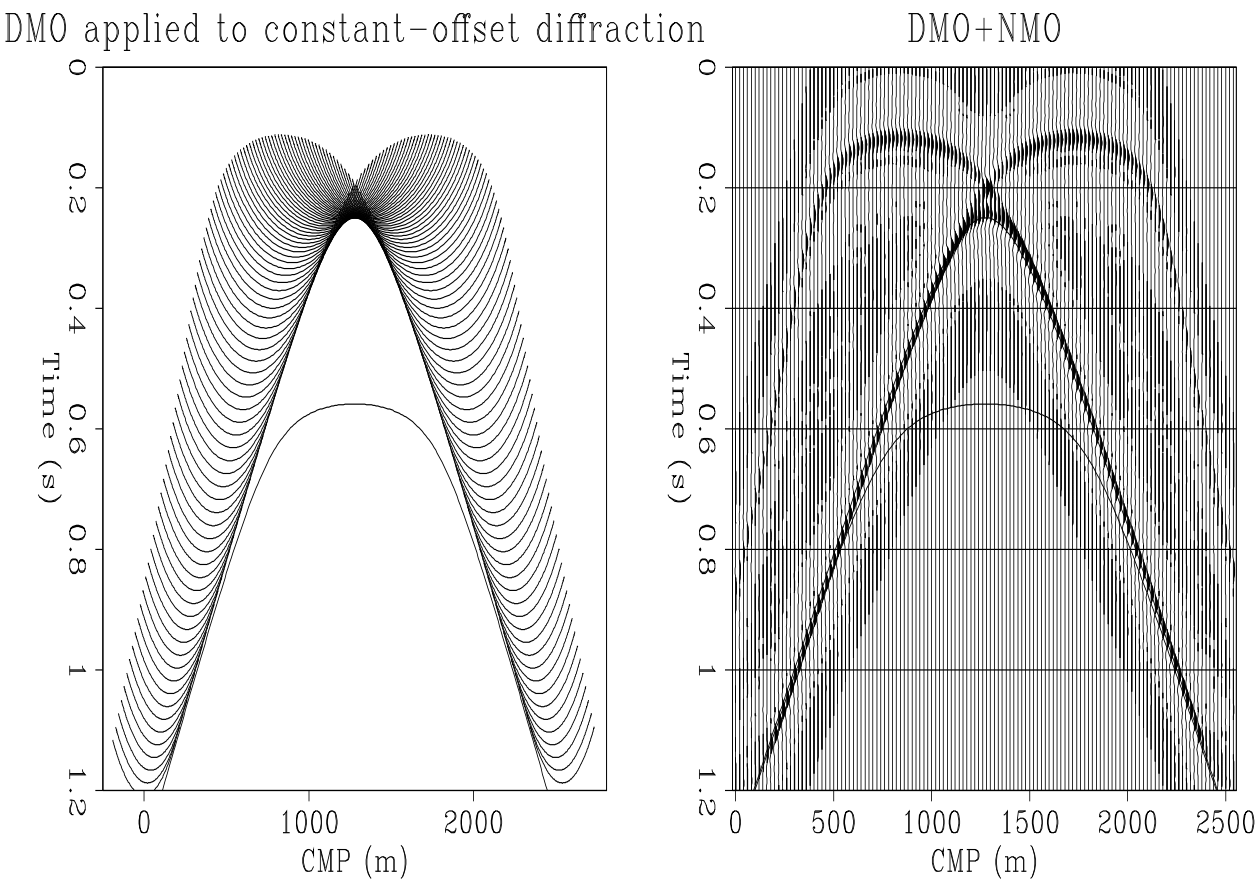

NMO $\cdot DMO$ kinematics; each point on the constant-offset diffraction curve is spread along the DMO curve and shifted with the NMO correction. [RIGHT] The result of applying $NMO \cdot DMO$ to the constant-offset hyperbola. The artifacts are due to using a constant amplitude along the DMO curve.]$NMO \cdot DMO$ transforms a constant-offset diffraction curve to a zero-offset hyperbola. [LEFT] $NMO \cdot DMO$ kinematics; each point on the constant-offset diffraction curve is spread along the DMO curve and shifted with the NMO correction. [RIGHT] The result of applying $NMO \cdot DMO$ to the constant-offset hyperbola. The artifacts are due to using a constant amplitude along the DMO curve.

Problem 2.

For the geometry presented in Figure ?? and using equation (??) show that the reflection point displacement measured along the reflector is

$$\mathbf{OR} = \frac{h^2}{v t_{cmp}} 2 \sin\theta \cos\theta$$

where t_{cmp} is the traveltime from the CMP location (point **F**) to the reflector and back (or the segment **FG** in time units) and v is the medium velocity. The length of the segment **FG** is given in equation (??). This equation appears in Levin's (1971) classic paper, and is also the first equation Dave Hale uses when explaining DMO in his SEG course notes.

REFERENCES

Deregowski, S. M., and Rocca, F., 1981, Geometrical optics and wave theory of constant-offset sections in layered media: Geophysical Prospecting, **29**, 374-406.

Deregowski, S. M., 1986, What is DMO?: First Break, **4**, 6-24.

Hale, I. D., 1983, Dip-moveout by Fourier transform: Ph.D. Thesis, Stanford University.

Hale, I. D., 1988, Dip-moveout processing: Course notes from SEG continuing education course, SEG.

Levin, F. K., 1971, Apparent velocity from dipping interface reflections: Geophysics, **36**, 510-516.

Popovici, A. M., and Biondi, B., 1989, Kinematics of prestack partial migration in a variable velocity medium: SEP – **61**, 133-147.

Yilmaz, O., and Claerbout, J. F., 1980, Prestack partial migration: Geophysics, **45**, 1753-1779.

DMO BY FOURIER TRANSFORM

2-D Fourier transforms of dipping events

In order to understand how DMO by Fourier transform works we have to examine some properties of the 2-D Fourier transform. In particular the fact that all events with a particular slope in the time-space domain are mapped to a single radial line (a line passing through the origin) in the frequency-wavenumber domain.

A two-dimensional function representing a segment of constant amplitude in a zero-offset section can be described by

$$H(y)\delta(\frac{t-t_0}{p}-y)$$

where

$$\begin{cases} H(y)=1; & y\in[a,b] \\ \\ H(y)=0; & y\in(-\infty,a)\cup(b,\infty) \end{cases}$$

where t and y are the zero-offset coordinates, t_0 is the intersection point on the time axis and the value p is the tangent of the slope

$$p=\tan\alpha=\frac{\Delta t}{\Delta y}.$$

In the corresponding depth model p becomes

$$p=\frac{\Delta t}{\Delta y}=\frac{2\sin\theta}{v}$$

as seen in Figure **??**. The angle θ represents the slope of the reflector in the depth model and v is the velocity of the medium. The function $\delta(\frac{t-t_0}{p}-y)$ has unitary amplitude when the argument is zero or $y=\frac{t-t_0}{p}$.

I include in the Appendix a formal derivation for the analytic solution of a 2-D Fourier transform of a constant length segment. The 2-D Fourier transform of an infinite segment is

$$\begin{aligned} S(\omega,k_y) &= \int dt\, e^{i\omega t}\int dy\, e^{-ik_y y}\delta(\frac{t-t_0}{p}-y) \\ \\ &= \int dt\, e^{i\omega t}e^{-ik_y\frac{t-t_0}{p}} \\ \\ &= e^{i\frac{k_y t_0}{p}}\delta(\omega-\frac{k_y}{p}) \end{aligned}$$

which in the ω, k_y space represents a line with slope

$$\frac{k_y}{\omega}=p=\frac{dt}{dy}=\frac{2\sin\theta}{v}. \tag{9}$$

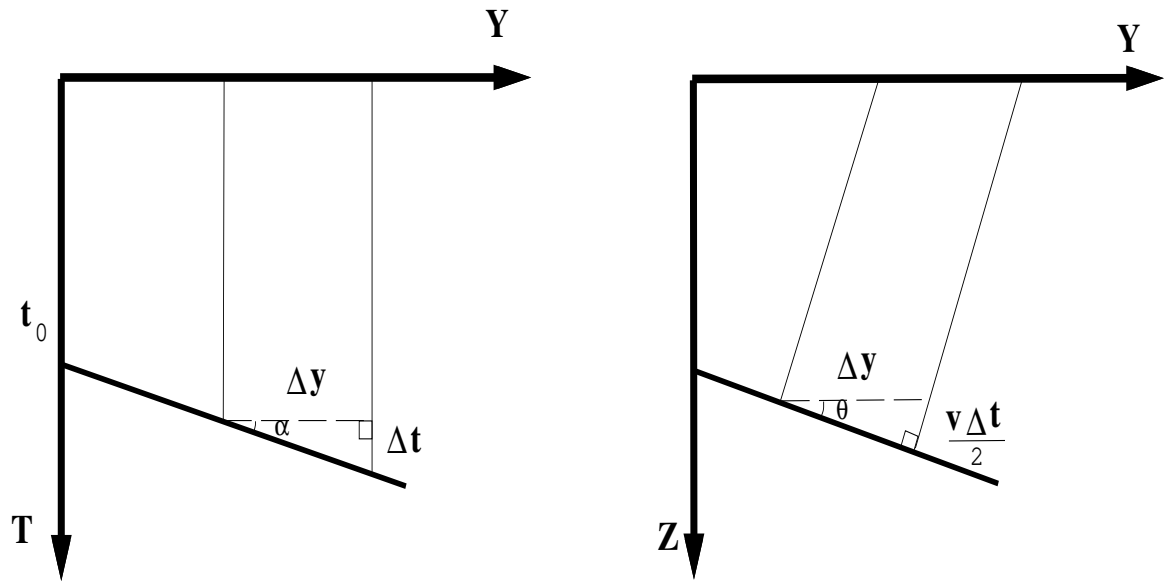

Figure 10: Dipping bed geometry in a constant-offset section and the corresponding constant velocity depth model. In a zero-offset section the slope of the reflection is $\Delta t/\Delta y = 2\sin\theta/v$, where θ is the dipping angle in the depth model and v is the velocity.

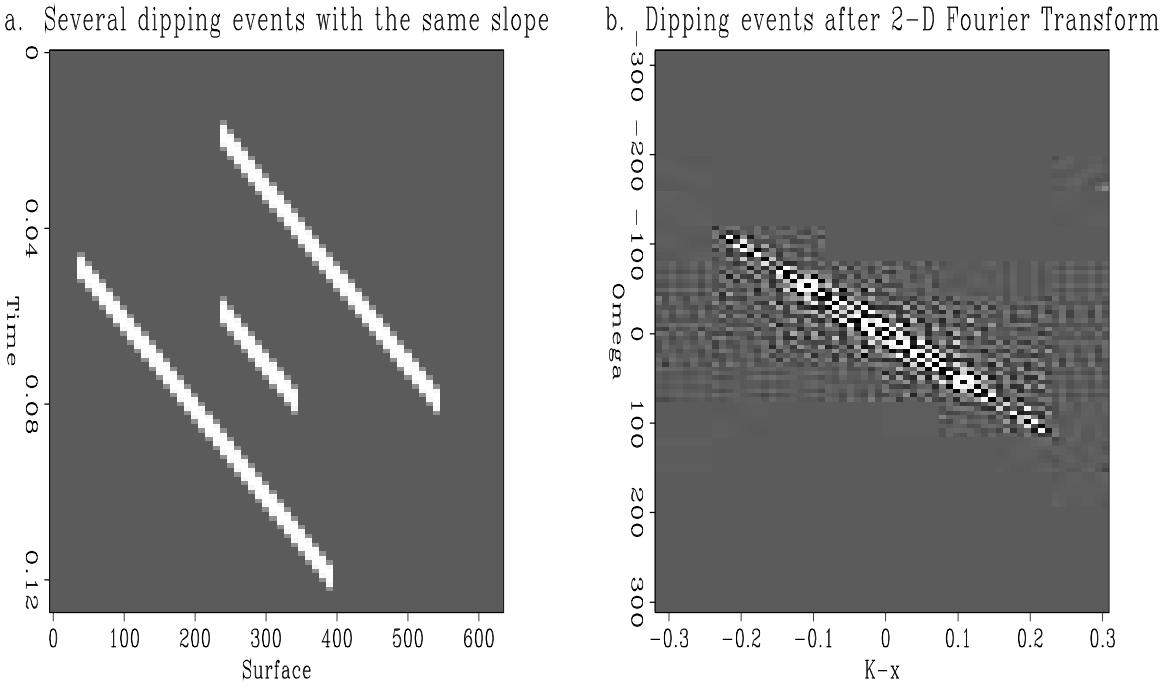

Figure 11: The effect of 2-D Fourier transform on events with same dip.
a. Several reflectors with the same dip in space-time coordinates.
b. The 2-D Fourier transform of the same section. Note that all the events are mapped on a radial line.

In Figure ??.a several dipping segments with the same slope are all mapped after the Fourier transformation to a radial line in Figure ??.b in ω, k_y space.

Hale's DMO

Given the geometry in Figure ?? we have proved in Part 1 that

$$t_0^2 = t_h^2 - \left(\frac{2h\cos\theta}{v}\right)^2 \tag{10}$$

where t_0 is the traveltime from CMP to the reflector and back, t_h is the source-receiver traveltime, $2h$ is the distance between source and receiver and v is the velocity of the medium. Note that in this situation the reflection point **R** in the nonzero-offset case differs from the actual reflection point **S** in the zero-offset case.

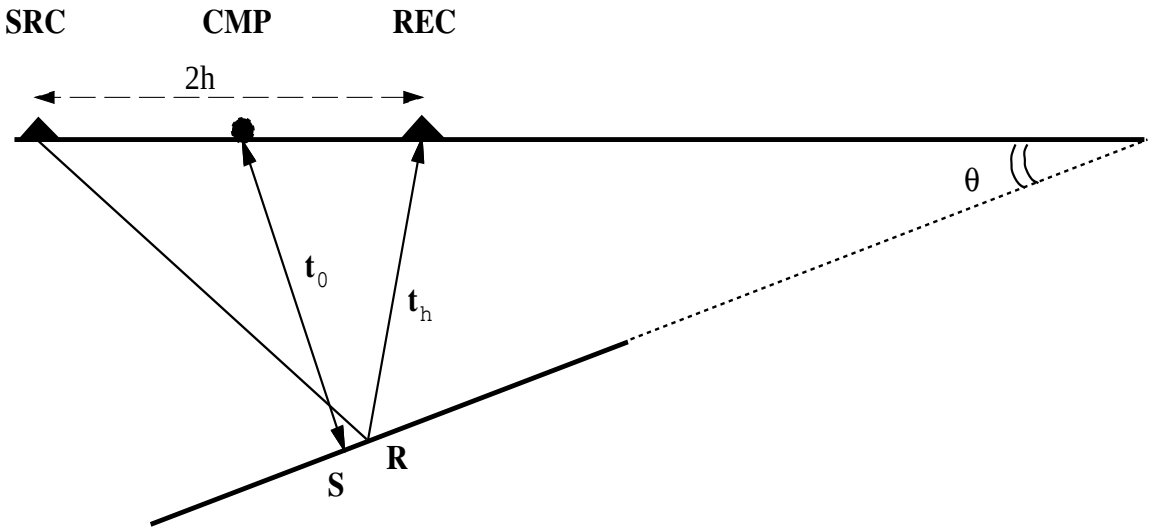

Figure 12: Geometry for a dipping reflector in a constant velocity medium. Notice that the reflection point for the nonzero-offset ray **R** is different from the zero-offset reflection point **S**. The dipping angle is θ.

Hale (1984) uses equation (10) to write

$$t_0^2 = t_h^2 - \frac{4h^2}{v^2} + \frac{4h^2\sin\theta^2}{v^2} \tag{11}$$

and we observe that the NMO corrected time is

$$t_n^2 = t_h^2 - \frac{4h^2}{v^2}. \tag{12}$$

Substituting t_n in equation (11) we have

$$t_0^2 = t_n^2 + \frac{4h^2\sin\theta^2}{v^2}. \tag{13}$$

Let us consider a pressure field $p(t_h, y, h)$ recorded as a function of nonzero-offset time t_h, midpoint y and offset h. In a constant-offset section we set the variable h to a constant value, so we have a 2-D field $p(t_h, y; h = h_0)$. For all the values of the offset h we have a 3-D field $p(t_h, y; h)$. We define a new field $p_n(t_n, y, h)$ as

$$p_n(t_n, y, h) \equiv p(\sqrt{t_n^2 + \frac{4h^2}{v^2}}, y, h) \tag{14}$$

obtained by replacing the value of the constant-offset traveltime t_h in $p(t_h, y, h)$ by its expression in equation (12)

$$t_h^2 = t_n^2 + \frac{4h^2}{v^2}.$$

Note that for a constant value of h this transformation amounts to shifting a value in a trace from t_h to t_n.

Next we define another field $p_0(t_0, y, h)$ as

$$p_0(t_0, y, h) \equiv p_n(\sqrt{t_0^2 - \frac{4h^2 \sin^2\theta}{v^2}}, y, h) \tag{15}$$

obtained by replacing the value of the NMO corrected traveltime t_n in $p_n(t_n, y, h)$ by its expression in equation (13). Equation (15) is dip dependent as it contains the variable $\sin\theta$. The new field $p_0(t_0, y, h)$ so far is unknown and further computations are needed to determine it. However equation (15) formally represents a mapping from a NMO corrected field to a DMO corrected field. Remember again that in this formulation the nonzero-offset reflection point **R** does not correspond to the zero-offset reflection point **S**.

So far in equation (15) the only variable that we cannot easily determine is $\sin\theta$ so we will try to find a transformation to express $\sin\theta$ as a function of other variables. We have in a zero-offset section

$$\sin\theta = \frac{v\Delta t_0}{2\Delta y}$$

as seen in Figure **??**. In equation (9) we proved that for a dipping segment we have

$$\frac{dt_0}{dy} = \frac{k_y}{\omega_0} = \frac{2\sin\theta}{v} \tag{16}$$

Now we need to Fourier transform the pressure field $p_0(t_0, y, h)$ to take advantage of the new variables k_y, ω that we used in equation (16). We have

$$P_0(\omega_0, k_y, h) = \int_{t_0} dt_0 \int_y dy e^{i(\omega_0 t_0 - k_y y)} p_0(t_0, y, h). \tag{17}$$

We can use the mapping we defined in equation (15) and replace $p_0(t_0, y, h)$ by $p_n(t_n, y, h)$ in equation (17). By changing the variable of integration we need to

calculate the Jacobian of the transformation (13). We have

$$t_0 = \sqrt{t_n^2 + h^2 \frac{k_y^2}{\omega_0^2}}$$

and

$$dt_0 = \frac{t_n}{\sqrt{t_n^2 + h^2 \frac{k_y^2}{\omega_0^2}}} dt_n. \tag{18}$$

We can now rewrite equation (17) as

$$P_0(\omega_0, k_y, h) = \int_{t_n} dt_n \int_y d_y \frac{t_n}{\sqrt{t_n^2 + h^2 \frac{k_y^2}{\omega_0^2}}} p_n(t_n, y, h) e^{i(\omega_0 \sqrt{t_n^2 + h^2 \frac{k_y^2}{\omega_0^2}} - k_y y)}, \tag{19}$$

which is Hale's DMO by Fourier transform.

Zhang's improved DMO

Zhang (1988) observed that in Hale's DMO the reflection point in the nonzero-offset case does not coincide with the reflection point in the zero-offset case. He shows a new formula for DMO which takes into account not only a time correction but also a mid-point correction.

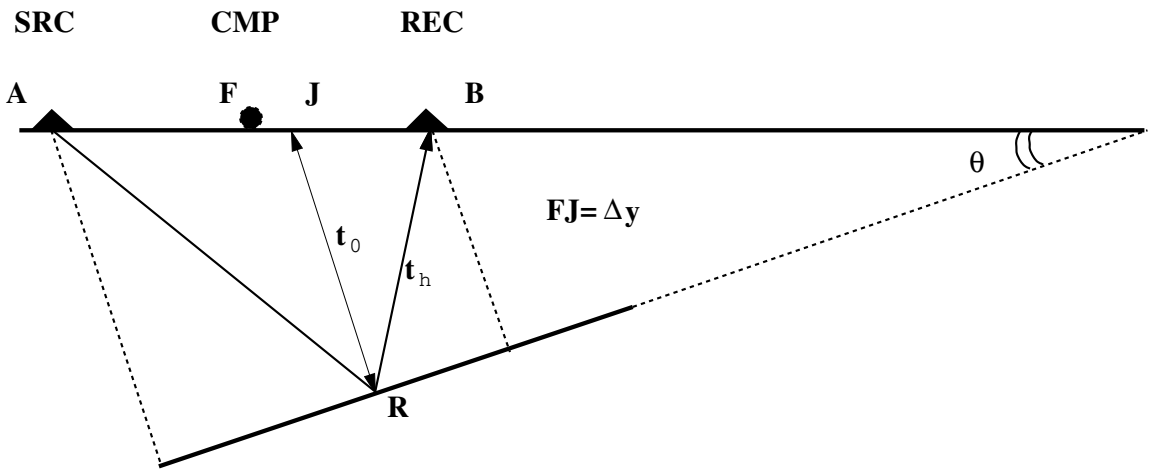

Figure 13: Geometry for a dipping reflector in a constant velocity medium. Notice that the reflection point for the nonzero-offset ray **R** is the same as the one for the zero-offset ray **JR**. The dipping angle is θ.

The $NMO \cdot DMO$ correction in constant velocity media as defined in Part 1 is

written

$$\begin{cases} \Delta y_0 = \dfrac{2h^2 \sin\theta}{v\sqrt{t_h^2 - 4h^2 \frac{\cos^2\theta}{v^2}}} \\ \\ t_0 = \dfrac{t_h^2 - \frac{4h^2}{v^2}}{\sqrt{t_h^2 - 4h^2 \frac{\cos^2\theta}{v^2}}}. \end{cases}$$

We can isolate the NMO transformation from equation (12) which is only a time-shift

$$t_n^2 = t_h^2 - \frac{4h^2}{v^2}$$

and write just for the DMO operator

$$\begin{cases} y_0 = y - \dfrac{2h^2 \sin\theta}{v\sqrt{t_n^2 + 4h^2 \frac{\sin^2\theta}{v^2}}} \\ \\ t_0 = \dfrac{t_n^2}{\sqrt{t_n^2 + 4h^2 \frac{\sin^2\theta}{v^2}}}. \end{cases} \tag{20}$$

To clarify the sign convention for the spatial coordinate in equation (20) note that the y axis is increasing to the left, and the angles are positive if they dip toward the right and negative if they dip toward the left. In Figure **??** the angle θ is negative. This can be also derived from equation (16)

$$\frac{dt_0}{dy_0} = \frac{2\sin\theta}{v}$$

where the sign of dy_0 determines the sign of the angle.

The next steps follow exactly Hale's reasoning by defining another field $p_0(t_0, y_0, h)$, with the addition that not only the time variable is changed but also the common-midpoint variable. This accounts for the fact that the DMO transformation defined by Zhang moves the nonzero-offset reflection point to a zero-offset reflection point. Stacking after this transformation produces true common depth point gathers. In the transformation defined by Hale, the reflection point for the nonzero-offset is different from the reflection point in the zero-offset case.

The Fourier transform of the new field is

$$P_0(\omega_0, k_{y_0}, h) = \int_{t_0} dt_0 \int_{y_0} dy_0 \; e^{i(\omega_0 t_0 - k_{y_0} y_0)} p_0(t_0, y_0, h). \tag{21}$$

We need to replace the variables t_0 and y_0 in equation (21) with the known variables t_n and y. Fortunately it is not necessary to express explicitly $t_n = t_n(t_0, y_0)$ and $y = y(t_0, y_0)$, though we assume the respective dependencies. From equation (20) we

can express the differentials of the new variables

$$\begin{cases} dy_0 = dy \\ \\ dt_0 = \dfrac{t_n(t_n^2 + 8h^2\frac{\sin^2\theta}{v^2})}{(t_n^2 + 4h^2\frac{\sin^2\theta}{v^2})^{\frac{3}{2}}} dt_n \end{cases} \tag{22}$$

and introduce them in equation (21). After using equation (16) to express

$$\frac{2\sin\theta}{v} = \frac{k_{y_0}}{\omega_0}$$

the phase becomes

$$\begin{aligned} \Phi &= \omega_0 t_0 - k_{y_0} y_0 \\ &= \omega_0 \frac{t_n^2}{\sqrt{t_n^2 + h^2\frac{k_{y0}^2}{\omega_0^2}}} - k_{y_0}(y - \frac{h^2 k_{y_0}}{\omega_0\sqrt{t_n^2 + h^2\frac{k_{y0}^2}{\omega_0^2}}}) \\ &= \omega_0\sqrt{t_n^2 + h^2\frac{k_{y_0}^2}{\omega_0^2}} - k_{y_0} y \end{aligned}$$

which should be noted is the same phase as in Hale's equation (19).

Equation (21) becomes

$$P_0(\omega_0, k_{y_0}, h) = \int_{t_n} dt_n \int_y dy \frac{t_n(t_n^2 + 2h^2\frac{k_{y0}^2}{\omega_0^2})}{(t_n^2 + h^2\frac{k_{y0}^2}{\omega_0^2})^{\frac{3}{2}}} p(t_n, y, h) e^{i(\omega_0\sqrt{t_n^2 + h^2\frac{k_{y0}^2}{\omega_0^2}} - k_{y_0} y)}. \tag{23}$$

Comparing equation (23) with Hale's equation (19) we notice that surprisingly the phase term is the same and the only difference is in the amplitude term. The two Jacobians are:

$$\begin{aligned} J_H &= \frac{t_n}{\sqrt{t_n^2 + h^2\frac{k_{y0}^2}{\omega_0^2}}} \\ \\ J_Z &= \frac{t_n(t_n^2 + 2h^2\frac{k_{y0}^2}{\omega_0^2})}{(t_n^2 + h^2\frac{k_{y0}^2}{\omega_0^2})^{\frac{3}{2}}}. \end{aligned}$$

The ratio between the two Jacobians is

$$\frac{J_Z}{J_H} = \frac{t_n^2 + 2h^2\frac{k_{y0}^2}{\omega_0^2}}{t_n^2 + h^2\frac{k_{y0}^2}{\omega_0^2}}. \tag{24}$$

MZO by Fourier transform

Both Hale and Zhang separate the NMO correction from the DMO correction. However for variable velocity media this can not be done, and in order to generalize the $NMO \cdot DMO$ operation we have to use the migration to zero-offset (MZO) concept. Migration to zero-offset is the process that transforms a nonzero-offset (constant offset) section into a zero-offset section. In constant velocity media $MZO = NMO \cdot DMO$. The Fourier transform expression is simply obtained by using again equation (20) without separating the NMO step. We have

$$\begin{cases} y_0 = y - \dfrac{2h^2 \sin\theta}{v\sqrt{t_h^2 - \frac{4h^2}{v^2} + 4h^2\frac{\sin^2\theta}{v^2}}} \\ \\ t_0 = \dfrac{t_h^2 - \frac{4h^2}{v^2}}{\sqrt{t_h^2 - \frac{4h^2}{v^2} + 4h^2\frac{\sin^2\theta}{v^2}}}. \end{cases} \tag{25}$$

The differentials of the new variables are

$$\begin{cases} dy_0 = dy \\ \\ dt_0 = \dfrac{t_h(t_h^2 - \frac{4h^2}{v^2} + 2h^2\frac{k_{y_0}^2}{\omega_0^2})}{(t_h^2 - \frac{4h^2}{v^2} + h^2\frac{k_{y_0}^2}{\omega_0^2})^{\frac{3}{2}}} dt_h \end{cases} \tag{26}$$

After replacing the variables y_0 and t_0 in equation (21) we obtain

$$P_0(\omega_0, k_{y_0}, h) = \int_{t_h} dt_h \int_y dy \frac{t_h(t_h^2 - \frac{4h^2}{v^2} + 2h^2\frac{k_{y_0}^2}{\omega_0^2})}{(t_h^2 - \frac{4h^2}{v^2} + h^2\frac{k_{y_0}^2}{\omega_0^2})^{\frac{3}{2}}} p(t_h, y, h)\, e^{i(\omega_0\sqrt{t_h^2 - \frac{4h^2}{v^2} + h^2\frac{k_{y_0}^2}{\omega_0^2}} - k_{y_0} y)}. \tag{27}$$

Note that if we replace the quantity

$$t_h^2 - \frac{4h^2}{v^2} = t_n^2$$

in equation (27) we get the same phase as the one obtained by Hale and Zhang, but the Jacobian differs from Zhang's Jacobian by a factor

$$\frac{J_M}{J_Z} = \frac{t_h}{t_n} = \sqrt{1 + \frac{4h^2}{v^2 t_n^2}} \tag{28}$$

which corresponds to the Jacobian of the NMO transformation.

REFERENCES

Claerbout, J. C., 1985, Imaging the Earth's Interior: Blackwell Scientific Publications.

Hale, I. D., 1983, Dip-moveout by Fourier transform: Ph.D. Thesis, Stanford University.

Hale, I. D., 1988, Dip-moveout processing: Course notes from SEG continuing education course, SEG.

Levin, F. K., 1971, Apparent velocity from dipping interface reflections: Geophysics, **36**, 510-516.

Popovici, A. M., and Biondi, B., 1989, Kinematics of prestack partial migration in a variable velocity medium: SEP – **61**, 133-147.

Yilmaz, O., and Claerbout, J. F., 1980, Prestack partial migration: Geophysics, **45**, 1753-1779.

Zhang, L., 1988, A new Jacobian for dip-moveout: SEP – **59**, 201-208.

APPENDIX A

The Fourier transform of a finite segment differs only in the amplitude term from the Fourier transform of an infinitely long segment. This is to be expected since we actually multiply the infinite segment by a boxcar filter which in Fourier domain means convolution with a sync function.

A two dimensional function representing a segment of constant amplitude in (t, y) space can be described by

$$H(y)\delta(\frac{t-t_0}{p} - y)$$

where

$$\begin{cases} H(y) = 1; & y \in [a, b] \\ \\ H(y) = 0; & y \in (-\infty, a) \cup (b, \infty) \end{cases}$$

where t and y are the coordinates, t_0 is the intersection point on the t axis and the value p is the tangent of the slope. The function $\delta(\frac{t-t_0}{p} - y)$ has unitary amplitude when the argument is zero or $t = t_0 + py$. The 2-D Fourier transform is

$$\begin{aligned} S(\omega, k_y) &= \int dt\, e^{i\omega t} \int dy\, e^{-ik_y y} H(y)\delta(\frac{t-t_0}{p} - y) \\ \\ &= \int dy\, H(y)\, e^{-ik_y y}\, e^{i\omega(t_0+py)} \\ \\ &= e^{i\omega t_0} \int_a^b e^{iy(\omega p - k_y)} \\ \\ &= e^{i\omega t_0} [\int_a^b \cos y(\omega p - k_y) + i \int_a^b \sin y(\omega p - k_y)] \end{aligned}$$

and using the well known trigonometric transformations

$$\begin{aligned} \sin\alpha - \sin\beta &= 2\sin\tfrac{\alpha-\beta}{2}\cos\tfrac{\alpha+\beta}{2}0 \\ \cos\alpha - \cos\beta &= -2\sin\tfrac{\alpha+\beta}{2}\sin\tfrac{\alpha-\beta}{2} \end{aligned}$$

we obtain

$$\begin{aligned} S(\omega,k_y) &= \frac{e^{i\omega t_0}}{\omega p-k_y}[\sin y(\omega p-k_y)|_a^b - i\cos y(\omega p-k_y)|_a^b] \\ &= \frac{e^{i\omega t_0}}{\omega p-k_y}2\sin\frac{b-a}{2}(\omega p-k_y)[\cos\frac{b+a}{2}(\omega p-k_y)+i\sin\frac{b+a}{2}(\omega p-k_y)] \\ &= \frac{e^{i\omega t_0}}{\omega p-k_y}2\sin\frac{b-a}{2}(\omega p-k_y)e^{\frac{b+a}{2}(\omega p-k_y)}. \end{aligned} \tag{A-1}$$